Critical points in the analysis of membrane pore structures by thermoporometry

F.P. Cuperus, D. Bargeman and C.A. Smolders

University of Twente, Faculty Chemical Technology, P.O. Box 217, NL-7500 AE Enschede (Netherlands)

Abstract

Several ultrafiltration membranes of the anisotropic and isotropic type were characterized by means of the thermoporometry. Successive cooling and heating runs were performed in order to investigate the effects of the water–ice and ice–water phase transitions on the structure of the membranes. The results found for membranes having different casting thicknesses indicate that, in some cases, pores in the sublayer of anisotropic UF membranes frustrate the measurement of the, for the separation, relevant pores present in the top layer.

Keywords: membrane preparation and structure; microporous and porous membranes; ultrafiltration; thermoporometry; membrane characterization

Introduction

Since the introduction of thermoporometry by Brun et al. in 1973, various porous structures have been examined by means of this technique, mainly by Brun et al. [1–7]. Most of these structures were of inorganic, ceramic nature although in the eighties a few organic swollen and non-swollen resins were investigated [5,6]. All the examined structures were of the isotropic type and the presence of a relatively high pore volume makes the pore size analysis by thermoporometry fairly simply. The success of thermoporometry in the systems used by Brun, brought several investigators to apply the technique for the characterization of po-

rous structures in the (wet) environment in which they are actually used. Desbrières et al. [8] measured pore size distributions of hemodialysis membranes, whereas Zeman and Tkacik [9] and Smolders and Vugteveen [10] used the method for the characterization of ultrafiltration (UF) membranes.

Ultrafiltration membranes are generally prepared from polymers; this enables one to manufacture porous membranes in a large area per volume ratio, i.e. in the form of flat sheets or hollow fibres. The main difference between these polymer systems and the porous ceramic media studied by Brun is the superior mechanical and chemical stability and the better definition of the morphological structure (in terms of pore size distribution) of the ceramic materials. Also, polymeric UF membranes are anisotropic: they consist of a thin skin layer with very small pores determining the performance

---

[1]Correspondence to: F.P. Cuperus, ATO Agrotechnologie, Agrotechnological Research Institute, P.O. Box 17, 6700 AA Wageningen, The Netherlands.

of the membrane and a thicker macroporous sublayer which provides the membrane with mechanical solidity. As the skin layer is very thin and its (surface) porosity generally is in the order of a few percent [11,12], the pore volume is low in comparison with ceramic membranes or catalysts. These aspects can have a large impact on the experimental procedure to be used and on the interpretation of the data found with thermoporometry.

Normally in the thermoporometry measurements of polymeric membranes, water is used as the liquid imbibed inside the pores, as this system of water filled pores has the closest resemblance with the practical situation. During the measurements, the water inside the pores will undergo a liquid–solid transition at least one time, a change of state which is accompanied by a volume expansion of the water. The question arises whether this phase transition changes the structure of the membrane in a reversible or in an irreversible way. For ceramics such a possible effect has never been mentioned, which confirms the assumed morphological stability of these materials. On the other hand, Brun suggests [4,5] that in a swollen resin in which the pore size in principle can change reversibly, different pore size distributions are found depending on the degree of swelling. The swollen membranes show broad distributions with sizes spreading over one order of magnitude, whereas the unswollen dry membranes analysed by the widely used method based on gas adsorption–desorption measurements, exhibit a very sharp pore size distribution.

Brun et al. [6] compared different characterization techniques by applying them to one and the same ceramic system. It appeared that results found with thermoporometry and gas adsorption–desorption hysteresis are consistent with one another. Similar agreement was found by Zeman and Tkacik [9] and Smolders and Vugteveen [10] when both methods were applied to polymeric ultrafiltration membranes. On the other hand, the thermoporometry results found by Zeman did not match with his SEM observations and could hardly explain the low cut-off values found for the same membranes, even when concentration-polarization effects were taken into account [13]. Consequently, Zeman suggests that by thermoporometry and gas adsorption–desorption the pores in the sublayer of the membrane are measured and therefore these methods do not give relevant information on the pores present in the skin. Smolders and Vugteveen found that the retention of components with molecular weights in the order of 10,000 Da was very low, which was not in agreement with the small pores found with thermoporometry. The conclusion must be that, although in some cases thermoporometry is a simple and effective method to determine the pore structure of certain porous media, for a number of particular systems, especially anisotropic polymeric membranes, doubtful results are found.

Theory

The basic principle of thermoporometry is the freezing (or melting) point depression which is due to the strong curvature of the solid–liquid interface present within small pores. A full thermodynamic description of this phenomenon is given by Brun et al. [1]. According to his treatise the size of a confined ice crystal is inversely proportional to the degree of undercooling (ΔT). Finely dispersed ice as present in a porous matrix therefore melts at temperatures below the ambient melting point of ice. The smallest size of the ice crystals or the smallest pore size that can be described properly is set by the validity of the assumptions made in the thermodynamic description of curved surfaces. For instance, the approximation of several properties of dispersed water by using values of normal, bulk water is limited to

volumes with characteristic radii larger than 1–2 nm. According to Defay and Prigogine [15] dispersed water at temperatures below $-50°C$ cannot be described anymore by using normal equilibrium thermodynamics. At such low temperatures any form of liquid water is instable and will become solid. This phenomenon can interfere with the 'normal' equilibrium freezing of water in very small pores (<2 nm). Monitoring cooling effects can also be disturbed by delayed nucleation of the ice phase inside the pores. This will be a minor effect when hydrophilic samples are analysed because the wetted membrane walls can act as nuclei and induce a fast liquid–solid transition [15]. However, for extremely hydrophobic materials delayed nucleation can influence the pore size analysis. Therefore the melting transition is preferred above the solidification for the pore size analysis, although the latter in principle should render identical information.

For the analysis of a porous substrate, the melting diagram (Fig. 1) can be monitored in a differential scanning calorimeter (DSC) and the pore size and pore volume are calculated from the equations derived by Brun. For the solid–liquid transition of water inside a cylindrical pore with radius r eqn. (1) holds. From the heat effect occurring during the transition, the pore volume at a certain undercooling (i.e. pore radius) is calculated. Equation (2) gives the heat of melting as a function of temperature, used in this procedure.
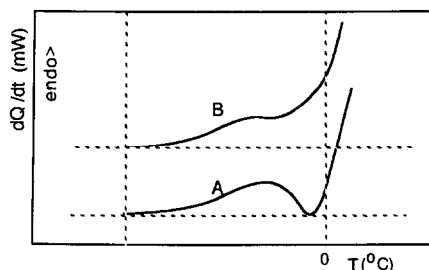
$$r = 0.68 - (32.33/\Delta T) \tag{1}$$

$$W_a = -0.155\Delta T^2 - 11.39\Delta T - 332 \tag{2}$$

Here r represents the pore radius (nm), ΔT the characteristic undercooling ($°C$), and W_a apparent transition energy (J/g).

Similar equations can be derived for the solidification process. These are not given here because only the melting process was used in the pore size analysis described in this paper.

As long as the pores have sizes between 2 nm and 25 nm, the shift of the freezing or melting points is large enough to be measured accurately. A typical example of a melting curve is given in Fig.1, curve A. Here, water inside the pores and 'free' water outside the membrane give rise to separate peaks and consequently the pore size distribution can be calculated easily. For some membrane types a deviant curve is found (see Fig. 1, curve B) and distributions calculated from such a curve remain questionable. This problem is discussed in more detail later-on in this paper (see: results and discussion).

Experimental

Both ceramic and polymeric membranes were investigated by means of thermoporometry. The ceramic γ-alumina systems were supplied by the inorganics group of our department and are described in the literature. According to gas adsorption–desorption and transmission electron microscopy these membranes have a well-defined pore structure and a porosity of ca. 50% [14]. Furthermore hollow fibre CA membranes used in blood filtration were analysed. According to literature these isotropic membranes exhibit a high porosity [8,16] which should make analysis by thermoporometry fairly simple.

Lab-made anisotropic ultrafiltration membranes were made of poly(2,6-dimethyl-1,4 phenylene oxide) (PPO), polysulfone (PSf)

Fig. 1. DSC thermogram as found for a narrow pore size distribution (A) and for a broad pore size distribution (B).

and cellulose acetate (CA). PPO membranes were prepared from a 10 wt.% polymer concentration in a mixture of trichloroethylene and 1-octanol in a weight ratio of 78/22. PSf membranes were cast from a solution composed of 15 wt.% PSf (P-3500 Union Carbide) in DMF. Flat CA membranes were made out of a 20 wt.% CA solution in 59 wt.% aceton, 19 wt.% demiwater and 2 wt.% magnesiumperchlorate. The solutions were cast on a glass plate at room temperature at thicknesses of 0.2 and 0.03 mm, respectively. In case of PPO, methanol was used as the coagulation bath, PSf and CA membranes were immersed in a water bath.

The calorimetric experiments were performed using a Perkin Elmer DSC 2 or DSC 4. First the sample with a total mass of ca. 50 mg (including water) was cooled at maximum speed to $-45\,°C$. After equilibrium was reached the heat effects during a controlled heating run at a scanning rate of $1\,°C/min$ were measured.

Pure water flux measurements were performed using freshly filtered RO water and a dead-end Amicon cell with a membrane area of 35 cm^2, at a pressure of 300 kPa. The steady state flux was determined after 3 hr of permeation.

Results and discussion

The effect of successive heating runs

γ-Alumina membranes and hollow fibre CA membranes exhibit a sharp pore size distribution (Figs. 2 and 3 respectively). The results found for the alumina membranes are in agreement with the data found with gas adsorption-desorption [14]. Alumina samples were analysed during several successive heating runs (up to 8 runs), but differences between the runs were not found. This means that this type of membrane is perfectly stable; the structure does not change during the analysis.

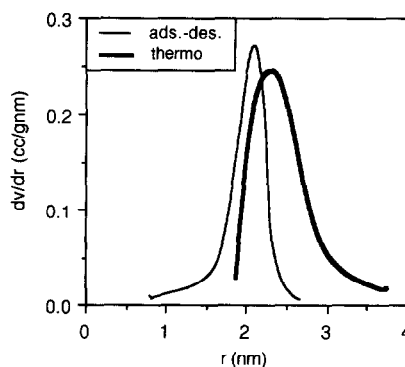In Fig. 3 pore size distributions for hollow fibre CA membranes, calculated from several

Fig. 2. Pore size distributions found for alumina membranes using thermoporometry and gas adsorption-desorption measurements (dv/dr: differential pore volume per g membrane).
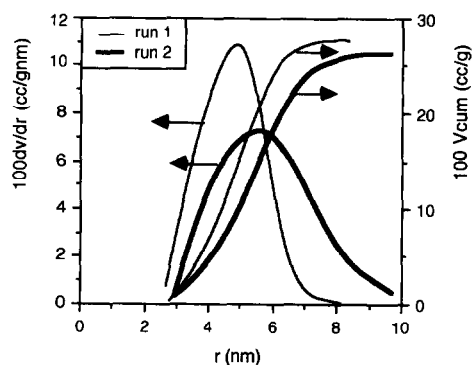

Fig. 3. Change in pore size distribution for hollow fibre CA membranes after two successive runs.

consecutive runs carried out with the same sample of membrane material, are shown. It appears that between the first and second run the pore size distribution shifts to slightly larger pore values. Differences between the following experiments are not significant. Obviously, the pore structure of the sample changes during or directly after the first two experiments but is stable thereafter. Probably this alteration has occurred during the cooling of the sample. Since the liquid–solid transition is accompanied by a volume expansion of 8–20% (dependent on the temperature and the pressure there exist different ice phases) [17,18], the nuclei deform the porous matrix to some extent. Because the

nuclei are induced within the original restricting pore space, the ultimate size of the crystal will only be a little larger than the nascent pore size. During the second cooling run the nuclei again deform the membrane matrix and enlarge the pore. Consequently the pore size measured in the second heating run is larger than that measured in the first run. From the volume expansion of the water the increase in pore size (for an 'original' pore of 5 nm) is calculated to range from 0.1 nm ($0°$C and 10^5 Pa) to 0.3 nm ($-35°$C and 2×10^8 Pa). Especially the latter value corresponds quite well with the experimental pore size increase. The fact that the volume expansion has to proceed in a confined pore space makes a transition accompanied by such a high pressure comprehensible. Nevertheless, the deformation appears to have reached its ultimate extent already after the second cooling step, since from the third run no change in the pore size distribution could be observed anymore. Probably the affine deformation caused by the water–ice transition stretches the pore walls to such an extent (reached after 2 transitions) that under the prevailing forces no further deformation is possible. The deformation of the original pore is not reversible because a relaxation phenomenon was not found; even after three days relaxation at $20°$C, the pore size distribution was identical with the previous (second) analysis run.

The pore size distribution of the thick PPO membranes determined by thermoporometry appeared to be very sharp (Fig. 4). All the pores have sizes between 1.5 and 4 nm and a maximum is found at ca. 2 nm. Figure 4 shows that the cumulative pore volume found in the first run is significantly lower than the value found (with the same sample) in the following runs. This remarkable difference suggests that not all the water present in the pores has been crystallized upon cooling during this first run but that at $-45°$C part of the water is present in
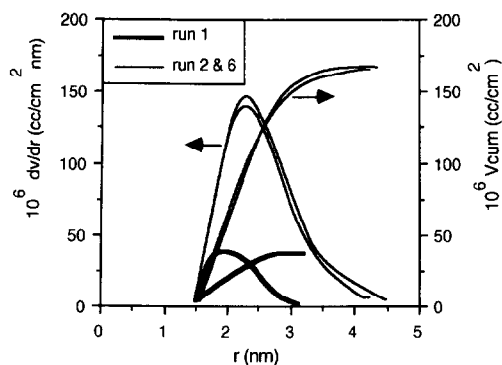

Fig. 4. Change in total pore volume (V_{cum}) for PPO membranes after several successive runs (casting thickness 0.2 mm; pore volume expressed as volume per unit membrane area).

the glassy state. This so-called vitrification occurs when the cooling rate has been so fast that nuclei could not be formed. However the extreme conditions needed for vitrification (cooling rates $> 10^6$ °C/sec) are certainly not present in the equipment used here, hence the presence of glassified water is not probable [19]. Since PPO is a hydrophobic material, heterogeneous nucleation induced by, e.g. the polymer wall is less probable than for hydrophilic materials. In the absence of other nuclei which could induce crystallization, homogeneous nucleation may be important. When homogeneous nucleation indeed should induce crystallization, the water (at $-45°$C) may be present as an undercooled liquid. According to the analysis of Defay and Prigogine [15], the homogeneous nucleation process at low temperatures is extremely slow and it might need several months to induce crystallization in all the pores of the membrane. This means that after cooling to $-45°$C, water can be present as an undercooled liquid instead of ice. Hence, phase transition (accompanied by a measurable heat effect) does not occur. The question is why during the second cooling run more ice is formed and crystallization appears to be less delayed. It should be expected that after the

heating run, all the ice has become water and the nucleation process then has to start all over again. Apparently, after the first heating run, conditions are permanently changed in a way that heterogeneous nucleation can take place in all the pores.

Another possible explanation for the observed increase in pore volume after the first heating run might be the presence of non-wetted pores, which become wetted after the first run. However, the origin of such non-wetted pores inside the membranes is hard to understand. Pores in UF membranes are formed by liquid–liquid demixing, which for PPO means that, in the native state, all the pores in the membrane are filled with methanol from the coagulation bath. The pores are filled with water by exchanging all the methanol, so in this way dry pores or 'de-wetting' of the membranes cannot be present. It may be that a trace of methanol is still present in some pores and could hinder crystallization, but also then it is not clear why during the second cooling run crystallization is more complete.

The structure of the top- and sublayer

The thermogram of a heating run executed with PPO membranes with a casting thickness of 0.20 mm shows two distinctly separated peaks (Fig. 1, curve A) and a simple calculation of the pore size distribution is possible. Other UF membranes, like the thick PSf and flat CA membranes, exhibit deviant melting curves like depicted in Fig. 1, curve B. Although in these latter cases the calculation of the pore size is possible, the resulting pore size distribution will be more questionable. Not only the impossibility to discriminate fully between 'pore peak' and 'free water peak' gives rise to doubtful results but also the precarious drawing of the base line. Furthermore it is not sure whether the larger pores, related to the higher melting temperatures, are present in the skin or in the sublayer. Especially in case of anisotropic membranes

which have relatively thick sublayers it can be imagined that going from the top to the bottom of the membrane a pore size gradient is present which leads to a melting curve with a shape as given in Fig. 1, curve B.

From the distribution obtained for PPO membranes (Fig. 4), the cumulative pore volume was calculated. Here, the total pore volume is expressed as volume per unit area of the top layer and for the thicker PPO membranes the values ranged from 5×10^{-5} till 20×10^{-5} cm^3/cm^2 and appeared to be strongly dependent on the casting thickness [10]. Because a PPO membrane is an anisotropic membrane, this pore volume is expected to be related to pores in the top layer. Consequently, the top layer thickness of the membrane can be calculated when a pore model is assumed. Recently, the top layer thickness of these PPO membranes, directly determined by a new method [20], was found to be ca. 0.2 μm. This result makes it questionable whether the pore volume measured with thermoporometry is only present in the skin. A simple calculation shows that a porosity value of more than 100% is needed to account for this volume to be present in a skin layer with a thickness of 0.2 μm. Hence, there are also small pores present in the sublayer of the membrane.

It has already been mentioned that the calculation of the pore size distributions of CA and PSf membranes from thermograms of the type shown in Fig. 1 (curve B) is cumbersome. From the anisotropic membrane concept one should expect that the small pores of the PSf and CA membranes are present in the skin. If this is really the case it is mainly because of the very low porosity of the skin [11,12] that the number of the pores or the cumulative volume in the skin cannot be measured. The smallest pore size can be found from the lowest temperature at which the thermogram (Fig. 1) deviates from the base line, but the larger pores in the sublayer make the complete analysis troublesome.

In order to diminish the influence of the sublayer pores, the ratio of the pore volume present in the skin to that in the sublayer was increased by preparing ultra thin PPO, CA and PSf membranes. For membranes with a casting thickness of 0.03 mm two separate peaks were found again and a pore size distribution could be calculated. The resulting distributions for CA and PSf membranes are given in Figs. 5 and 6, respectively. The distributions are considerably broader than the pore size distributions found for the thicker PPO membranes (Fig. 4).

The broad pore size distribution found for the thin (0.03 mm) PPO membranes (Fig. 7) completely deviates from the characteristic sharp

Fig. 7. Comparison of PPO membranes with casting thicknesses 0.03 mm and 0.20 mm. (scale dv/dr 0.20 mm membranes should be multiplied by 10, see also Fig. 4).

TABLE 1

Flux and pore volume as determined by thermoporometry for various membranes

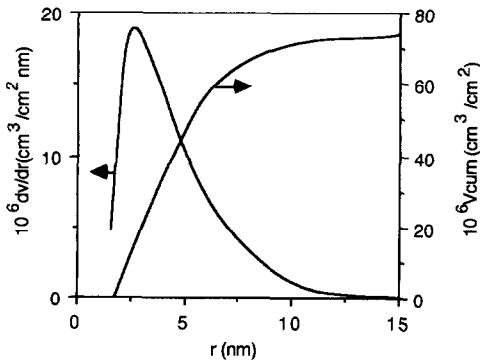| Membrane type	PPO		PSf		CA	
Casting thickness (mm)	0.2	0.03	0.2	0.03	0.2	0.03
Flux (cm/hr-bar) (± 1)	1	2	3	30	8	4
$10^5 \ V_{cum}$ (cm^3/cm^2) ($\pm 30\%$)	5-20	3	?	4	?	5

Fig. 5. Pore size distribution of thin CA membranes (casting thickness 0.03 mm, pore volume expressed as volume per unit membrane area).
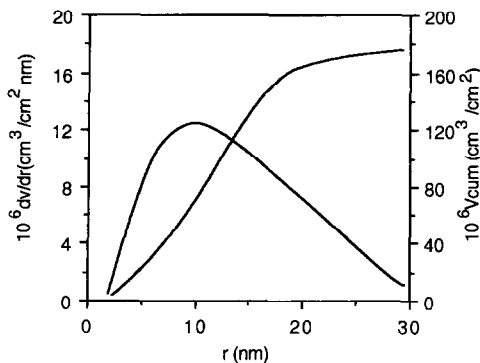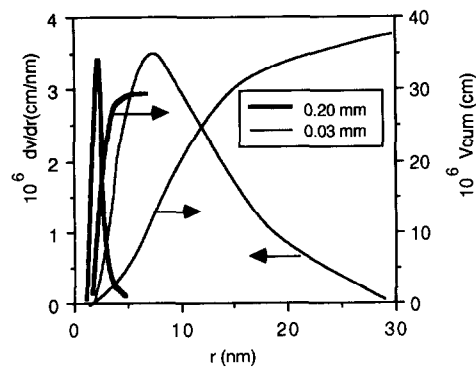

Fig. 6. Pore size distribution of thin PSf membranes (casting thickness 0.03 mm, pore volume expressed as volume per unit membrane area).

peak exhibited by the thick (0.20 mm) PPO membranes. This difference in pore size distribution between the thin and the thick PPO membranes suggests a change in membrane structure caused by a change in casting thickness. Now the question arises whether the results found for the PSf and CA membranes are biased by the change of the casting thickness. To investigate this possibility, the pure water flux of the thin and thick membranes (of CA, PSf and PPO) was measured. The results are given in Table 1.

The pure water fluxes of both PPO membrane types are surprisingly close to each other. This does not only imply that the pore structure of both types is similar but also supports the idea of the predominant role of the top layer

in this case. On the other hand, it can be argued that the small pores found by thermoporometry in thicker PPO membranes are not all related to pores in the skin. The number of pores that do determine the performance is so small that they cannot be measured by thermoporometry [11,12]. The thin membranes used are assumed to have a higher ratio of pore volume in the skin to pore volume in the sublayer than the thick membranes, but this is only due to a thicker sublayer. A DSC-sample of a thin membrane therefore contains about '10 times more' skin than a sample of a thick membrane, which makes the detection of the pores in the skin easier. Consequently the pore size distribution found for the thin membranes is expected to be a better representation of the actual distribution of the pores in the skin. Or in other words: the real pore size distribution in the skin of thick PPO membranes resembles the pore size distribution found for the thin membranes. For the CA and PSf membranes significant differences in flux values are found for different membrane thicknesses.

The increase in the flux value for thin PSf membranes might imply that the structure of the membrane has been changed, e.g. the average pore size has increased or the skin thickness has decreased or a combination of these two effects has occurred. It can also be argued that for these membranes the sublayer has a substantial resistance for transport. The existence of a pore gradient from the skin to the bottom of the membrane, which could contribute to this resistance was indicated by other methods too [10,20,21]. When such a gradient does exist in both thin and thick membranes, the effect of using thin membranes in thermoporometry might be that the larger pores (> 30 nm) which are present at the bottom of the thick membranes are missing in the thin membrane. The tenfold increase of the water flux, however, can hardly be explained in this way and it must be concluded that the decrease in membrane thickness resulted in a change of pore size as well.

The flux of the 0.20 mm CA membranes is higher than that of the 0.03 mm membranes. This can only be explained by a change in pore structure. Consequently, CA membranes of different casting thickness cannot be compared.

Conclusions

It has been shown that thermoporometry can be a very effective method for the characterization of porous media. However, for anisotropic polymeric membranes the method cannot be used without certain restrictions. Because the whole membrane, i.e. top layer and sublayer structure which both can contain pores of comparable size, is analysed, it is sometimes difficult to decide whether a measured pore size distribution corresponds to pores in the sublayer or to pores in the skin [21,22]. Furthermore, the very low porosity of the skin frustrates the accurate determination of the pore size distribution.

The smallest pore that can be analysed properly by thermoporometry is ca. 2 nm. The limits are set by the assumptions made in the thermodynamic description of the process which are no longer valid for temperatures lower than −40°C. The upper limit, or the largest pore that can be determined successfully by thermoporometry, is set by the effect of the curvature on the freezing point depression. For pores of 30 nm or larger the shift from the ambient fusing point is so small that the effect cannot be separated from the free water peak and accurate determination of pore radius and pore volume is not possible anymore.

References

1   M. Brun, A. Lallemand, J.F. Quinson and Ch. Eyraud, Changements d'état liquide solide dans les milieux poreux I–III, J. Chim. Phys., 70 (1973) 973.

2 M. Brun, A. Lallemand, J.F. Quinson and Ch. Eyraud, A new method for the simultaneous determination of the size and the shape of the pores: the thermoporometry, Thermochim. Acta, 21 (1977) 59.

3 M. Brun, J.F. Quinson and L. Benoist, Determination of pore size distributions by DSC, Thermochim. Acta, 49 (1981) 49.

4 M. Brun, J.F. Quinson and R. Spitz, Caracterisation texturale par thermoporometrie et par adsorption–desorption d'azote de resin d'état gonflé, Macromol. Chem., 183 (1982) 1523.

5 M. Brun, J.F. Quinson and R. Blanc, Caracterisation texturale des resins en milieu reactionel par thermoporometrie, Macromol. Chem., 181 (1981) 873.

6 Ch. Eyraud, J.F. Quinson and M. Brun, The role of thermoporometry in the characterization of porous solids, in: K.K. Unger, J. Rouquerol, K.S.W. Sing and H. Kral (Eds.), Characterization of Porous Solids, Elsevier, Amsterdam, 1988, p. 295.

7 Ch. Eyraud, J.F. Quinson and M. Brun, Progress in thermoporometry, in: K.K. Unger, J. Rouquerol, K.S.W. Sing and H. Kral (Eds.), Characterization of Porous Solids, Elsevier, Amsterdam, 1988, p. 307.

8 J. Desbrières, M. Rinando and M. Brun, Relation entre le taux de retention et la distribution des pores dans une membrane d'UF, J. Chim. Phys., 78 (1981) 187.

9 L. Zeman and G. Tkacik, Pore volume distribution in UF membranes, in: D.R. Lloyd (Ed.), Materials Science of Synthetic Membranes, ACS Symp. Ser. No. 269, American Chemical Society, Washington, DC, 1985, p. 339.

10 C.A. Smolders and E. Vugteveen, New characterization methods for asymmetric UF membranes, in: D.R. Lloyd (Ed.), Materials Science of Synthetic Membranes, ACS Symp. Ser. No. 269, American Chemical Society, Washington, DC, 1985, p. 329.

11 A.G. Fane, C.J.D. Fell and A.G. Waters, The relationship between surface pore characteristics and flux for UF membranes, J. Membrane, Sci., 9 (1981) 245.

12 U. Merin and M. Cheryan, A study of the fouling phenomena during ultrafiltration of cottage cheese whey, J. Appl. Pol. Sci., 2 (1980) 2139.

13 L. Zeman and G. Tkacik, Characterization of porous sublayers by thermoporometry, J. Membrane Sci., 32 (1987) 329.

14 A. Leenaars, Ceramic membranes, Thesis University of Twente, The Netherlands, 1984.

15 R. Defay and I. Prigogine, Surface Tension and Adsorption: The Effect of Curvature on the Triple Point, Longmans, New York, NY, 1966, p. 244.

16 T. Kobayashi, M. Todoki, M. Kimura, Y. Fujii, T. Takeyama and H. Tanzawa, Characterization of UF membranes, in: E. Drioli and M. Nakayaki (Eds.), Membranes and Membrane Processes, Plenum Press, New York, NY, 1986, pp. 25-33.

17 Handbook of Chemistry and Physics, 58th edn., R.C. Weast (Ed.), CRC Press, Boca Raton, FL, 1977.

18 International Critical Tables, 1st edn., Vol. iv, E.W. Washburn (Ed.), Mc Graw Hill, New York, NY, 1928.

19 R.H. Lange and J. Blödorn, Das Elektronenmikroskop, Thieme Verlag, Stuttgart, 1981, Chap. 9, pp. 192-201.

20 F.P. Cuperus, D. Bargeman and C.A. Smolders, A new method to determine the skin thickness of asymmetric UF membranes using colloidal particles, J. Colloid Interface Sci., 135 (1990) 486.

21 F.P. Cuperus, Characterization of UF membranes: Pore structure and top layer thickness, Thesis University of Twente, The Netherlands, 1990.

22 F.P. Cuperus and C.A. Smolders, Characterization of UF membranes: membrane characteristics and characterization techniques, Adv. Colloid Interface Sci., 34 (1991) 135.